When true colors still shine through: LC-MS-based metabolomics study of fabrics dyed with European buckthorn (Rhamnus cathartica) berries after accelerated light ageing

Marine Chambaud, Lindsay Mas-Normand, Céline Joliot, Carole Mathe, Olivier Dangles, Gérald Culioli

Dyes and Pigments 249 (2026) 113625

Contents lists available at ScienceDirect

Dyes and Pigments

journal homepage: www.elsevier.com/locate/dyepig

When true colors still shine through: LC-MS-based metabolomics study of fabrics dyed with European buckthorn (*Rhamnus cathartica*) berries after accelerated light ageing

Marine Chambaud [a,1], Lindsay Mas-Normand [a,1], Céline Joliot [a], Carole Mathe [a], Olivier Dangles [b], Gérald Culioli [a,*]

[a] IMBE, Aix Marseille University, Avignon University, CNRS, IRD, Avignon, France
[b] SQPOV, INRAE, Avignon University, Avignon, France

ARTICLE INFO

Keywords:
Metabolomics
LC-MS
Rhamnus cathartica
Light-induced ageing
Flavonoids
Anthraquinones

ABSTRACT

Since prehistoric times, humans have used dye-producing plants to color textiles, artworks, and ritual objects. Yellow-yielding species have been especially important due to their availability and the chemical stability of many of their flavonoid-based colorants. Among them, *Rhamnus* species (buckthorns) are notable for producing yellow to greenish hues from their flavonoid-rich berries. These long-standing practices inform modern research on natural colorants, phytochemistry, and sustainable textile science.

In this context, this study investigates the chemical and chromatic evolution of cotton fabrics dyed with *Rhamnus cathartica* (European buckthorn) berries when subjected to accelerated light ageing. Fabrics were exposed to xenon-lamp irradiation equivalent to 3, 30, and 300 years of museum-type light. Color fading was assessed by CIELAB colorimetry, and dye degradation was analyzed using LC-DAD and untargeted LC-MS-based metabolomics. Colorimetric data showed rapid fading, fabrics appearing even whiter than undyed samples after the 300-year equivalent exposure. LC-DAD analysis revealed a drastic decline of most coloring compounds, including flavonoids and anthraquinones, which became undetectable in the most aged samples, highlighting the limited sensitivity of LC-DAD for heavily degraded textiles. In contrast, LC-MS metabolomics enabled the detection and putative annotation of 25 dye molecules, mainly flavonoid glycosides and anthraquinones. Molecular networking highlighted distinct structural families, and surprisingly many dye-related compounds remained detectable even in fully bleached fabrics.

These results demonstrated that LC-MS-based metabolomics can constitute a powerful tool for identifying residual dyes in historical textiles, supporting conservation and reconstruction of ancient dyeing practices.

1. Introduction

Dyes degradation can make their identification in historical textiles difficult and bias conclusions on how the color originally looked and what plants were used for dyeing [1]. The study of the degradation of molecules used as taxonomic markers of dye plants is currently of great interest in archeological research [2]. Providing insight to what remains once color has disappeared can help with dye identification, as well as preservation and restauration of ancient textiles [1].

In an analytical point of view, liquid chromatography coupled to tandem high-resolution mass spectrometry (LC-HRMS/MS) provides great separation and enables a fairly accurate characterization of individual chemical components in complex mixtures. It has become one of the most commonly used analytical tools to study both ancient textiles and modern reference dyed samples [3,4]. The study of dye degradation over time [2] or after accelerated ageing under heat [5] or light [1,6,7] provides valuable insights into the kinetics and the chemical markers of dye degradation. For example, in previous studies photo-ageing experiments have led to the identification of several hydroxybenzoic acid derivatives as degradation products of flavonoids in historical dyes [1,7,8]. Such knowledge can be used to assist the identification of the dye source and/or to adjust preservation conditions in museums [6,9,10]. In

* Corresponding author.
E-mail addresses: gerald.culioli@univ-avignon.fr, gerald.culioli@imbe.fr (G. Culioli).
[1] First authors.

https://doi.org/10.1016/j.dyepig.2026.113625
Received 5 December 2025; Received in revised form 30 January 2026; Accepted 30 January 2026
Available online 4 February 2026

addition to applications in heritage chemistry, natural dyes are experiencing a renewed surge of interest. Thus, plant-based dyes are being reintroduced to replace synthetic dyestuff deemed harmful to the environment and human health [11]. Over the last decades, studies have also focused on the production of functional textiles with antioxidant, antimicrobial or UV-protective properties using plant dyes [11].

Metabolomics, the youngest of the "omics" sciences, is commonly defined as permitting the comprehensive study of the whole set of low-molecular weight molecules (referred to as 'metabolites') within a biological or chemical sample [12]. Metabolomics aims at identifying and quantifying the diverse range of compounds produced in a sample, offering a global snapshot of its chemical composition. In the field of cultural heritage and archaeology, metabolomics constitutes a powerful approach for the analysis of complex organic materials found in artworks and historical artefacts [13–15]. Thus, while traditional analytical approaches may fail to detect all components or differentiate between closely related substances, metabolomics can be a powerful tool for the study of complex mixtures of natural compounds such as organic dyes [16]. Indeed, LC-MS-based metabolomics can enable the detection of a wide range of chemical compounds of natural dye extracts, including minor constituents and degradation products, providing insights into the origin, composition, and ageing processes. This information is crucial for developing conservation strategies and for reconstructing historical techniques used by artisans. Metabolomics can also be used to assess the variation of composition between plant species, organs, physiological state, growth conditions or localization [17,18]. Therefore, in the long term, this type of analytical approach has the potential to unlock precious information from ancient artefacts that so far remains unattainable.

Rhamnaceae are flowering plants distributed almost worldwide comprising 55 genera [19]. The hydroalcoholic extracts from berries of most Rhamnaceae contain rhamnetin, a flavonoid also found in extracts of many different plants. This compound, as well as other flavonols, is particularly prevalent within yellow dye plants of the genus *Rhamnus* [20]. Depending on the fruit maturity and the dyeing parameters (pH and temperature of the dye bath, type of mordant etc.), buckthorn berries (*Rhamnus* spp.) can give a yellow, green or purple-red color [20,21]. This is due to its unusual phytochemical profile as buckthorn berries contains both flavonols and anthraquinones, in glycosylated or aglycone forms [22]. More specifically, European buckthorn (*Rhamnus cathartica* L.) have been commonly used as a textile dye in the Mediterranean region since the Middle Ages [22].

In this context, this work focused on the evolution of the color and chemical composition of a textile dyed with berries of *R. cathartica* after light-induced accelerated ageing. Previously such treatments have been used to study the ageing of dyes and dyed fabrics and establish degradation pathways and kinetics [1,23,24]. Here, the unaged and aged fabrics were first characterized using CIELAB colorimetry and LC-DAD. Then, a LC-MS based metabolomics approach was used to analyze the whole composition of dyes and study its evolution from the unaged fabrics to the fully light-faded fabrics. Detected dyes were then annotated using MS/MS fragmentation data and molecular networking. The aim of this study was to provide a strategy to study degraded textiles that no longer show their original color.

2. Material and methods

2.1. Plant material and chemicals

Ripe dried European buckthorn (*Rhamnus cathartica* L.) berries were purchased from Kremer Pigmente (Aichstetten, Germany). Ultrapure water was produced on a Purelab flex from Elga Labwater (High Wycombe, U.K.) for the extraction and on a Synergy UV purification system from Merck Millipore (Darmstadt, Germany) for chromatographic analyses. Aluminum potassium sulfate dodecahydrate (alum) came from Acros organics (Geel, Belgium), ethylenediaminetetraacetic acid (EDTA) from Applichem Gmbh (Darmstadt, Germany) and anhydrous sodium carbonate from Fluka (Neu-Ulm, Germany). LC-MS-grade methanol (MeOH) was purchased from PanReac AppliChem (Monza, Italy), LC-MS-grade formic acid (FA) from Fisher Chemical (Illkirch, France) and LC-MS grade acetonitrile from Carlo Erba Reagents (Val de Reuil, France).

2.2. Preparation of the fabrics and dyeing process

The cotton fabric was prepared using protocols adapted from Cardon [22] and Marquet [25]. The cotton fabric was first cleaned and boiled-out using a three-step process: (i) the fabric was immersed in 4 L of boiling tap water containing soap (20 g/100 g of fabric) and sodium carbonate (2.23 g/100 g of fabric) for 2 h under agitation, (ii) after rinsing and air drying, the fabric was dampened with lukewarm water, and then immersed in softened water containing soap (20 g/100 g of fabric) and heated at 60 °C under agitation for 30 min, and (iii) the fabric was rinsed using tap water at 30 °C and then 60 °C, immersed in hot tap water (60 °C) for 30 min, rinsed with softened water, and air-dried.

For mordanting, the cotton fabric was immersed in 4 L of softened water containing alum (20 g/100 g of fabric) and heated upon 100 °C for 1 h under agitation. It was left in the solution to cool down overnight and then subjected to a second step of mordanting with a gallnut extract. For this step, 4 L of softened water containing gallnut powder (30 g/100 g of fabric) were heated at 100 °C. The fabric was added to the boiling solution and stirred for 2 h. The cooled-down fabric was then rinsed with softened water, soaked in the alum-based mordanting bath for 2h, rinsed again with softened water and air-dried.

Three samples measuring 10 cm × 8 cm were cut out from the mordanted fabric, weighted precisely and dyed separately using the following process: i) *R. cathartica* berries were ground using an A11 basic analytical mill from IKA (Staufen, Germany) and the exact same mass of powdered *R. cathartica* berries as the dyed fabric sample (approximately 1.3 g) was extracted in 1 L of softened water at room temperature for 30 min and then heated at 90 °C for 1 h, ii) the resulting dyeing bath was cooled down and filtered, iii) the fabric sample was added to the dyeing bath and heated at 90 °C for 1 h, and iv) the dyed fabric was rinsed with softened water and air-dried. A blank fabric (BF) was obtained using the same process without the dye plant.

2.3. Accelerated light ageing of dyed fabrics and monitoring of their fading

Artificial light-induced ageing was performed using a SUNTEST CPS+ from Atlas (Linsengericht, Germany) equipped with a xenon 1500 W lamp, and two filters (coated quartz and special window glass) allowing a 310-800 nm irradiation range. The irradiance was set to 765 W/m^2 (corresponding to approximately 174 klx) and the temperature of the ageing chamber was kept under 60 °C. Each fabric sample was cut into four identical pieces. One was left unexposed while the others were exposed to irradiation for 8 h (1.4 Mlx.h), 78 h (13.6 Mlx.h) or 773 h (134.5 Mlx.h). As light exposure (lx.h) is the product of illuminance (lx) and time (h), this treatment equates to an exposition for 8 h a day at 150 lx for 3, 30 or 300 years, respectively. The fabric samples were named T_0, T_1, T_2 or T_3 according to the accelerated ageing to which they were subjected (0, 3, 30 or 300 years, respectively).

The fading of the fabrics was monitored through the measurement of their CIELAB coordinates (L*a*b*), using a CM2300d spectrophotometer from Konica Minolta (Tokyo, Japan). The resulting data were acquired and treated with the Spectra Magix NX (vers. 3.4) software. This method allowed an objective and uniform assessment of the fading of each dyed sample. The Euclidean distance (dE*) between the CIELAB coordinates of each aged sample and the corresponding unaged sample was then calculated (Eq. 1) [26].

$$dE^* = \sqrt{(\Delta L^*)^2 + (\Delta a^*)^2 + (\Delta b^*)^2} \quad \text{Eq. 1}$$

One-Way ANOVA and post-hoc Tukey HSD tests were performed to determine if the differences observed between the ageing groups were significant or not.

2.4. Chromatographic analyses of the dyed fabrics

A 0.5 × 0.5 cm sample of each fabric was extracted using an ultrasound-assisted method adapted from Zhang [27] and Lech [28]. Each sample (approximately 5.5 mg) was put in 500 µL of MeOH/-FA/EDTA (89:5:6, v/v/v) and sonicated in a PEX1 N extractor from REUS (Drap, France) at 24 kHz for 10 min and then heated at 60 °C for 25 min. After 5 min of centrifugation at 4660 *g* on a Frontier 5515 centrifuge from Ohaus (Nänikon, Switzerland), the supernatant was evaporated to dryness under N_2 at 40 °C and precisely weighted. Each sample was then solubilized in 500 µL of MeOH/H_2O (1:1, v/v) and filtered on a PTFE 0.2 µm syringe filter (VWR, Radnor, PA, USA). Quality Control (QC) samples were obtained by transferring 40 µL of each sample to a first vial (QC_0) and then transferring 80 µL of QC_0 into each of 8 other vials (QC_1.QC_8).

Chromatographic analyses were performed using parameters optimized for the analysis of yellow dye plants [16]. UPLC-DAD analyses (referred to as LC-DAD in the rest of the text) were performed on an Acquity UPLC I-Class system (Waters, Milford, USA) equipped with a DAD detector set to 200-700 nm with a resolution of 1.2 nm. The separation was performed on a Kinetex C18 column (2.1 × 100 mm, 1.7 µm core-shell particles; Phenomenex, Cheshire, U.K.) and mobile phase eluents were water (A) and acetonitrile (B), both acidified by 0.1% FA. A gradient elution (15 % B for 1 min, then 15-100 % B in 10 min, maintained for 2.5 min before re-equilibrating for 2.5 min) was achieved at 35 °C with a flow rate of 0.4 mL/min. The injection volume was 5 µL for all samples.

UPLC-HRMS/MS (referred to as LC-MS in the rest of the text) experiments were done using the same chromatographic conditions as for LC-DAD analysis. The chromatographic system was connected to a SYNAPT G2-Si Q-TOF mass spectrometer equipped with an electrospray ionization source (ESI) operating in negative mode. The following MS source parameters were used: capillary voltage 1 kV, sampling cone 40 V, source offset 80 V, source temperature 120 °C, desolvation temperature 450 °C, cone gas flow 50 L/h, desolvation gas flow 850 L/h and nebulizer 6.5 bars. Continuum data were acquired in Fast DDA (data-dependent acquisition) using the resolution resolving mode. Mass spectra were summed during 0.2 s in the *m/z* range 50-1200. Five precursor ions with an intensity threshold of 5E03 were fragmented using a collision energy ramp from 10 to 40 V (*m/z* 50) to 40-70 V (*m/z* 1200). Precursor ions were excluded for 6 s after fragmentation and fragment ions were scanned during 0.1 s. The 20 most intense ions from analytical blank samples were compiled in an exclusion list.

QC_0 was injected 10 times before the analytical sequence. Samples and blank samples were then injected in randomized order, with a QC inserted every 5 samples and two analytical blanks (MeOH/H_2O, 1:1, v/v) at the beginning and the end of the analytical sequence.

A semi-quantitative approach was also used to determine which compounds were still detected after the longest light ageing treatment (T_3). Two tables containing the peak intensity in LC-DAD and LC-MS data of compounds annotated as **UV1**-**UV16** (dyes detected in LC-DAD) for each ageing group were built. Then, a threshold corresponding to the limit of detection (LOD calculated as 3 times the noise level) was applied to each table. For LC-DAD data, the noise was determined as 1E02 and for LC-MS data as 1E03. Venn diagrams of UV-detected compounds and of MS-detected compounds were obtained from these two sets of data using InteractiVenn [29].

2.5. Data processing of LC-MS data and statistical analyses

The raw data were converted into ".mzML" files using Msconvert (Proteowizard, vers. 3) [30] and then an open access script [31] was used to correct the lockmass. Data processing was handled on MZmine vers. 4.5.20 [32] using parameters that are detailed in the Supplementary Table S1. A first data matrix was built and then filtered by applying a subtraction step using blanks. This step removed contaminants detected in analytical blanks and also *m/z* features found in blank samples (coming from undyed fabrics) to obtain the final data matrix.

The statistical analysis of these metabolomics data was conducted on the online platform MetaboAnalyst vers. 6.0 [33]. Briefly, the data was normalized using the fabric weight of each sample and then $\log_{10}$ transformation and auto-scaling were applied. Principal component analysis (PCA), hierarchical clustering analysis (HCA) and heatmap (both using euclidean distance and Ward clustering) were used to visualize and interpret the data.

2.6. Molecular networking and putative annotation of chemomarkers

The molecular network was constructed using the Feature-Based Molecular Networking (FBMN) tool from GNPS [34] using the following parameters: mass tolerance: 0.02 Da, minimum cosine score: 0.70, and minimum matched fragment ions: 6. Cytoscape vers. 3.10.3 [35] was then used to visualize and edit the molecular network.

Molecular formulas were calculated using the Molecular Formula Calculator from MSTools. SIRIUS vers. 6.1.1 was used for compound class prediction using CANOPUS and structure database [36,37]. All annotations were then verified manually by comparison with the literature in terms of MS/MS fragmentation pattern and previous description in *Rhamnus* species. This whole workflow led to a confidence level 2 of annotation, which corresponded to a putative identification of *m/z* features on the basis of MS/MS match with databases and/or literature data [38].

3. Results and discussion

3.1. Global assessment by colorimetry and LC-DAD of the impact of accelerated light ageing on the dyed fabrics

Dyed cotton samples initially had a warm yellow color, but as expected, their color visibly and quickly faded after light exposure (Fig. 1A). CIELAB colorimetry was used to describe objectively the color and its evolution. In the CIELAB color space, the L* value measures the lightness of the sample, from 0 (black) to 100 (white). The a* (green-red axis) and b* (blue-yellow axis) values give the direction of the color. Therefore, positive a* and b* values represent colors that tend toward red and yellow, respectively [39]. The mean L* value of samples increased gradually upon accelerated light ageing from 74.1 ± 2.2 (for T_0 samples) to 93.1 ± 0.2 (for T_3 samples) highlighting the whitening effect of light exposure. It should be noted that T_3 samples had a higher L* value than the unaged BF sample (89.1), showing that the aged dyed fabrics were whiter than the unaged undyed one. Simultaneously, a* and b* values declined from 4.4 ± 0.5 and 37.4 ± 2.6 (for T_0 samples) to −0.5 ± 0.1 and 5.0 ± 0.5 (for T_3 samples), respectively, showing the loss of reds and yellows that resulted in a visible greying of the color (Fig. 1B).

To assess the color fading, the euclidean distances (dE) between the color of each aged samples and the corresponding unaged samples were calculated (Fig. 1C). Guidelines for museum conservation describe the color variation and associated light exposure for colored materials in four different categories of sensitivity to light. Two thresholds have been established, the "Just Noticeable Difference" (JND), corresponding to dE = 1.8, and the almost total fade that is estimated to 30-100 times the JND [40]. For highly photosensitive samples such as plant dyes, the light dose corresponding to a JND is estimated between 0.22 and 1.5 Mlx.h

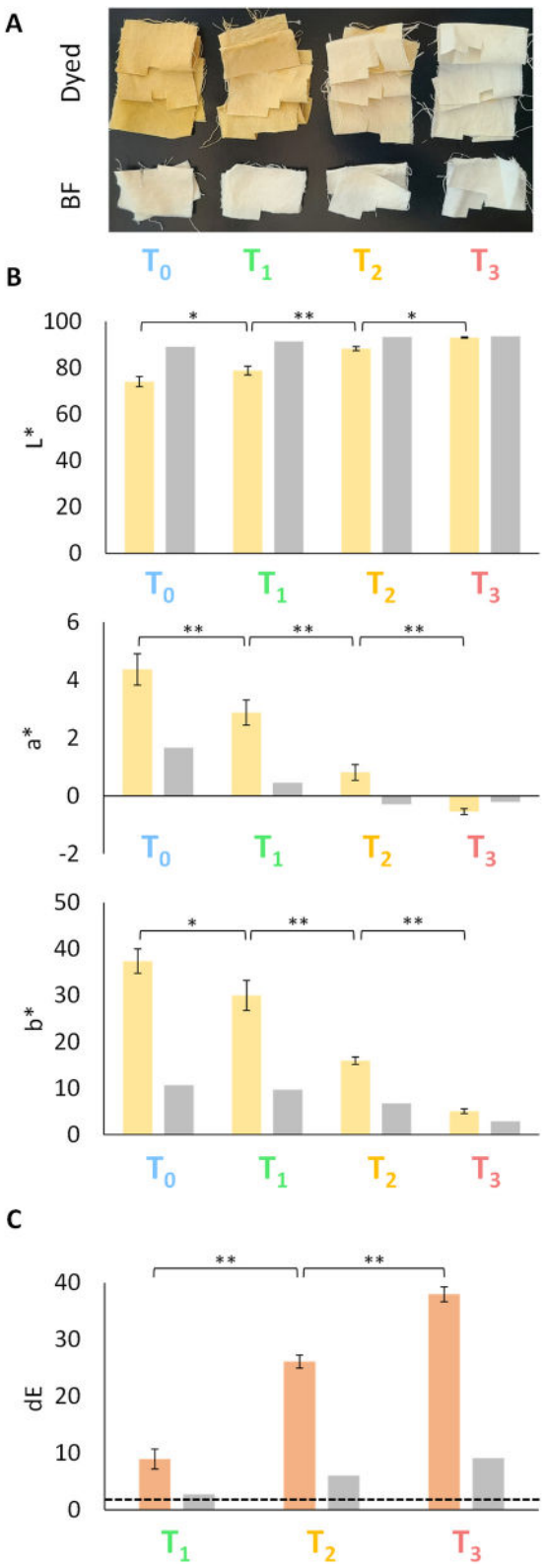

Fig. 1. (**A**) Photographs of all cotton fabrics (BF: Blank fabrics). (**B**) Mean L*, a*, and b* values of dyed (yellow) and BF (grey) samples after each ageing treatment. (**C**) dE calculated between aged (T_1: eq. 3 years, T_2: eq. 30 years, and T_3: eq. 300 years) and unaged (T_0) samples of dyed fabrics (orange) and BF (grey). The dE value considered as "Just Noticeable Difference" (JND is displayed as a dashed line. * and ** showed statistically different *p*-values with $p < 0.05$ and $p < 0.01$, respectively. (For interpretation of the references to color in this figure legend, the reader is referred to the Web version of this article.)

when the light spectrum includes the UV range, which corresponds to a 150 lx exposure 8 h a day for half a year to 3.5 years (Fig. 1C) [40]. The first ageing treatment used in this study was set to 1.4 Mlx.h, or a 3-year exposure under the described conditions, so T_1 samples represented the JND phase of ageing. From this, T_2 samples (13.6 Mlx.h, 30 years) were chosen as an intermediary phase between JND and almost total fade, and T_3 samples were treated with a dose 100 times higher than T_1 (134.5 Mlx.h, 300 years) to represent fully faded fabrics (Fig. 1C).

The mean dE for T_1 samples was 9.0 ± 1.8, which is already above JND. T_2 and T_3 samples displayed a dE from unaged samples of 26.1 ± 1.2 and 38.0 ± 1.3, respectively (Fig. 1C). These results showed that the color of dyed cotton samples was greatly affected by light. The shortest exposure resulted in a color difference that exceeded the expected result for a just noticeable fade. This could be explained by the chosen dose, as it was in the upper range for JND. Additionally, high temperatures (up to 60 °C in this experiment) are known to accelerate the degradation of organic compounds, leading to color loss [5,40]. On the other hand, the longest treatment resulted as expected in an almost total fade. Thus, samples were aged under harsh conditions, the longest experiment (T_3) resulting in whiter fabrics than the initial undyed ones (BF).

The fading of extracts indicated a loss of dye content in the fabrics. The degradation rates of dye compounds were assessed using LC-DAD. A decomplexation step first enabled the recovery of the dye extracts from the dyed cotton fabric samples. As *R. cathartica* contains glycosylated flavonoids, mostly flavonols, and anthraquinones, a soft decomplexation method inspired by Zhang [27] and Lech [28] was used to extract dyes from the fabric without breaking glycosidic bonds. Thus, instead of the conventional extraction with a boiling hydrochloric acid solution, a two-steps extraction consisting of 10 min of ultrasound-assisted extraction at room temperature followed by heating at 60 °C was performed in MeOH/FA/EDTA (89:5:6, v/v/v). The detection and semi-quantification of compounds were conducted at 350 nm and 450 nm, i.e. at the wavelengths of maximal absorption for flavonoids and anthraquinones, respectively [41]. A total of 12 flavonoids (**UV_{1-12}**) and 4 anthraquinones (**UV_{13-16}**) were detected by LC-DAD in the unaged (T_0) extracts (Fig. 2).

The peak area of each detected chromatographic peak was measured in all extracts (T_0-T_3) and normalized using the weight of the corresponding fabrics (Supplementary Table S2). The total area of all the chromatographic peaks corresponding to flavonoids decreased by 32% from T_0 to T_1. In T_2 extracts, only 7% of the sum of the total peak areas of flavonoids remained while no flavonoids were detected in T_3 extracts. Interestingly, the normalized area of one flavonoid (**UV_5**) first increased from T_0 to T_1, indicating it might be a degradation product of another compound (Supplementary Table S2).

Anthraquinones were detected in T_0 extracts at concentrations lower that the LOQ. Although semi-quantification was not possible, it should be noted that their concentrations decreased during the ageing treatment, as no anthraquinones (values < LOD) were detected in T_1, T_2 and T_3 extracts (Supplementary Table S2). These results explained the rapid fading of fabrics, as most dyes were no longer detected in T_2 and T_3 extracts. These results showed that LC-DAD, an analytical technique commonly used to study dyes in historical samples, would not be sensitive enough to detect, let alone identify, compounds from samples as severely faded as those under conditions T_2 and T_3.

3.2. LC-MS-based metabolomics approach

3.2.1. Chemical discrimination between aged and unaged fabrics

LC-MS is a sensitive method that enables the detection, identification and semi-quantification of a broad range of compounds without the need of standards. It is commonly used to study ancient dyed textiles, often in combination with LC-DAD [42,43]. Untargeted LC-MS-based metabolomics approaches offer high throughput processes based on statistical tools and open databases that facilitate and deepen the exploration of such complex data and the annotation of compounds of

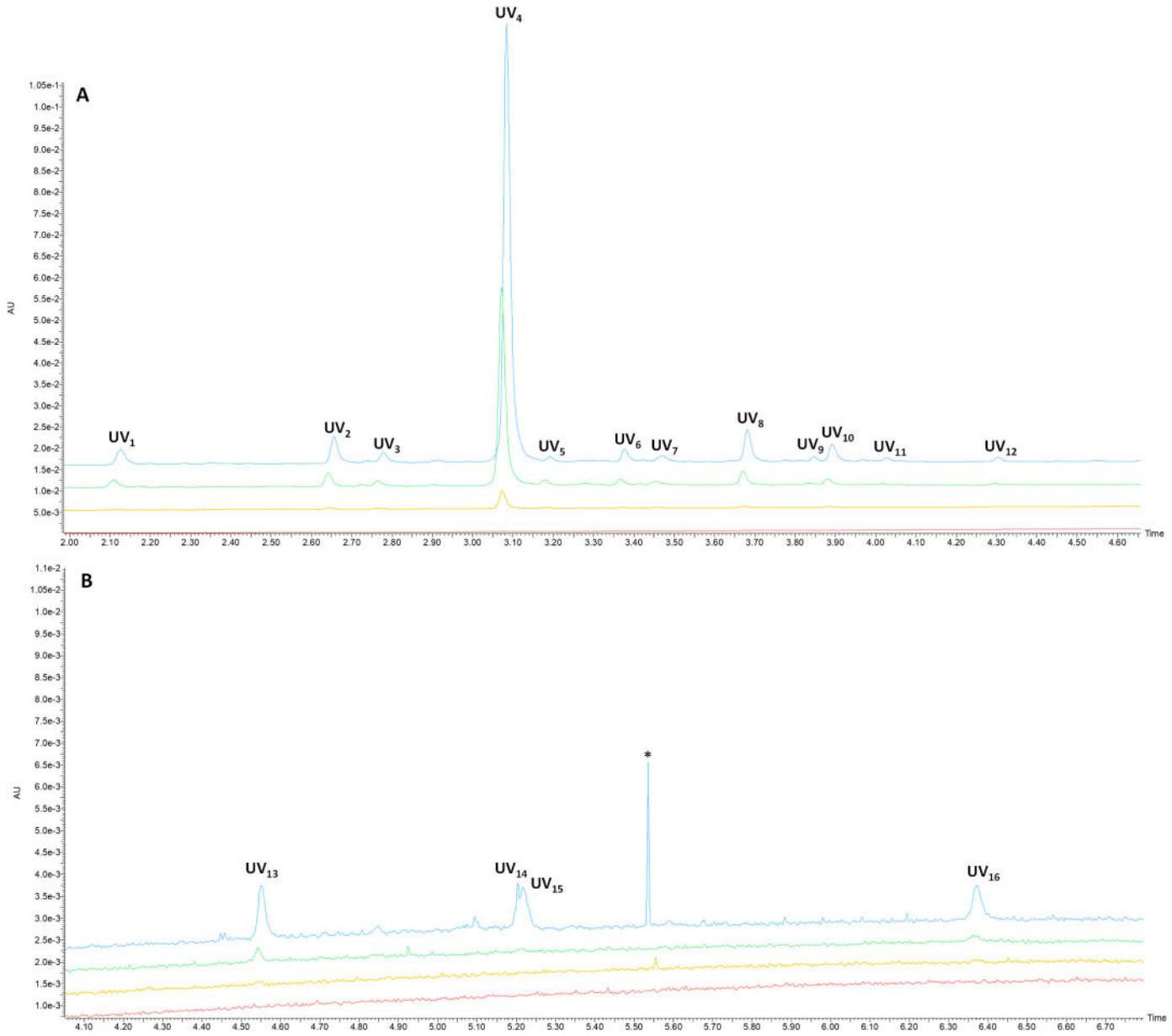

Fig. 2. LC-DAD chromatograms (**A**) at 350 nm (specific to flavonoids) and (**B**) at 450 nm (specific to anthraquinones) of extracts of aged (T_1: eq. 3 years in green, T_2: eq. 30 years in yellow, and T_3: eq. 300 years in red) and unaged (T_0, in blue) fabrics dyed with *R. cathartica* berries. Detected compounds are annotated as **UV_1** to **UV_{16}**. *Artefact peak. (For interpretation of the references to color in this figure legend, the reader is referred to the Web version of this article.)

interest. In this work, all extracts were analyzed using a LC-MS metabolomics approach previously optimized on a panel of fourteen yellow dye plants [16]. Data processing was performed using MZmine, an open-source software, and led to a list of 372 *m/z* features. The statistical analysis conducted on this feature list did not show a satisfactory discrimination between samples (Supplementary Fig. S1A). Moreover, BF samples were statistically closer to the dyed samples of the corresponding fabrics group than to each other. This result led to the hypothesis that a wide number of *m/z* features came from the fabric itself instead of the dye plant (Supplementary Fig. S1B). To correct that, blank subtraction steps were added to the process leading to a final list including 95 relevant *m/z* features.

Unsupervised multivariate statistics, more particularly principal component analysis (PCA), hierarchical clustering and heatmap were used to understand the effect of accelerated light ageing on the phytochemical composition of the dyed fabrics. PCA reduces the dimensionality of the data, thus enabling its visualization. Hierarchical clustering shows the structure of the data and helps identify groups within samples. Finally, heatmap represents the values of variables using different colors to display the structure of the data matrix [44]. The final feature list, previously normalized using the extracted fabric weights, was loaded in MetaboAnalyst 6.0 where $\log_{10}$ transformation and auto-scaling of the data were performed. Hierarchical clustering performed on this feature list showed that BF samples were clustered with T_3 samples, rather than with dyed samples of the same fabrics group as it was observed with the complete dataset (Supplementary Fig. S2). This indicated that this T_3+BF group is most likely characterized by a lack of specific chemical markers.

Once the data was validated, a PCA was performed on dyed samples only (BF and QC samples were excluded) (Fig. 3A). On the resulting PCA score plot, principal components 1 (PC1) and 2 (PC2) explained 72.2% and 18.1% of the total variance, respectively. T_0 samples were separated from T_1 samples along PC2, while other sample groups (T_2 and T_3 conditions) were separated along PC1, highlighting a drastic

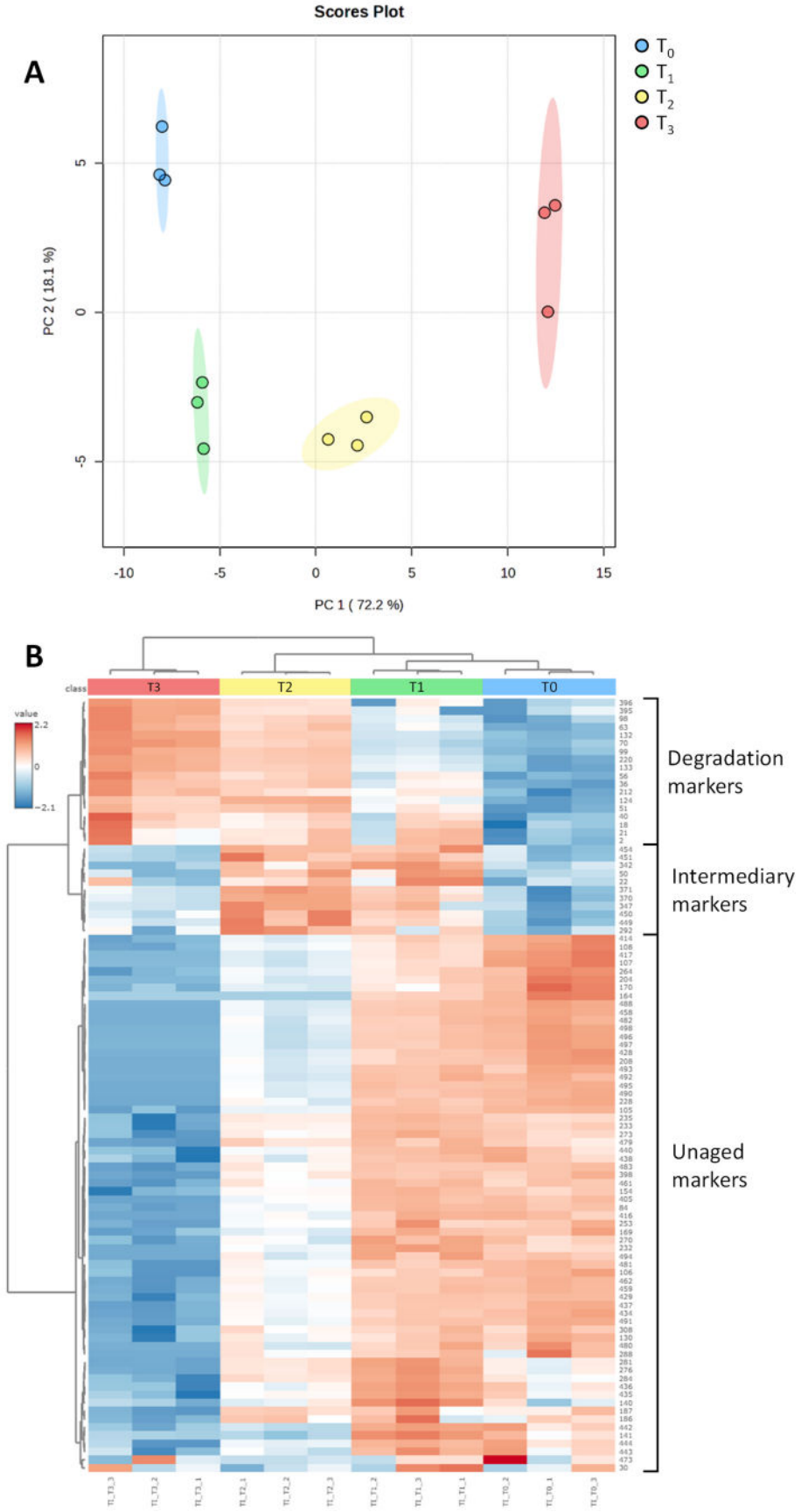

Fig. 3. Visualization using unsupervised multivariate statistics of the LC-MS dataset obtained from extracts of aged (T_1: eq. 3 years, T_2: eq. 30 years, and T_3: eq. 300 years) and unaged (T_0) dyed with *R. cathartica* berries. (**A**) PCA score plot; (**B**) Heatmap showing the relative intensity of each *m/z* feature in each sample group, labelled with their feature list ID (See Supplementary Table S3).

composition change after the ageing period T_1. These data showed a gradient of ageing, ranging from samples with little fading (T_1 condition) to those that underwent drastically longer light ageing and were strongly or even completely faded (T_2 and T_3 conditions, respectively). These results are in accordance with those obtained using CIELAB colorimetry and LC-DAD.

As the feature list was rather small (95 *m/z* features) and already highly processed, all *m/z* features were considered relevant to the study. A heatmap was then constructed to classify features according to their intensity in each ageing group (Fig. 3B). The resulting heatmap highlighted three groups of *m/z* features: (i) chemical markers of unaged or slightly faded fabrics specific to T_0 and T_1 conditions ("unaged markers"), (ii) chemical markers of intermediary aged fabrics specific to T_1 and T_2 conditions ("intermediary markers"), and (iii) chemical markers of strongly or even completely faded fabrics specific to T_2 and T_3 conditions ("degradation markers"). The majority of the *m/z* features detected (66 out of 95) were unaged markers, which showed that there were few markers specific to aged samples (T_2 or T_3).

3.2.2. Dyes annotation

From the 95 *m/z* features, 13 were identified as fragments, adducts or isotopes from other features. As such, they were considered artefacts and not further annotated. The molecular class of all other *m/z* features was predicted using CANOPUS. Interestingly, most features (46 out of 95) were classified as fatty acid derivatives, regardless the ageing group. Moreover, 21 *m/z* features were classified as flavonoids, and four as anthraquinones. Only these 25 *m/z* features (numbered from **1** to **25**) were annotated further. However, the full *m/z* feature list containing heatmap groups, different identifiers used in the article, results from class prediction and annotations, is available in Supplementary Table S3.

The annotation was conducted by comparing the molecular formula and MS/MS fragmentation pattern to the literature for the genus *Rhamnus* and multiple databases (LOTUS, Pubchem and KNapSack). Table 1 summarizes the retention time, *m/z* values, MS/MS fragmentation data and putative identification of the annotated compounds. Other compounds were annotated as fatty acid derivatives and artefacts, comprising all features that were not identified as molecular ions (fragments, adducts and isotopes). Thus, non-dye compounds were not considered specific to *R. cathartica* and will not be discussed further as they would not enable the identification of the dye plant if found in a historical sample.

Also, a feature-based molecular network workflow was conducted on the GNPS online platform and the resulting network was visualized using Cytoscape (Fig. 4). Molecular networking enables the visualization of the whole dataset based on the similarity of MS/MS fragmentation

Table 1
Putative annotation of flavonoids and anthraquinones detected by LC-(-)-ESI-MS and LC-DAD in the extracts obtained from both aged and unaged fabrics dyed with berries of *R. cathartica*.

Annotation ID	UV ID	Retention time (min)	*m/z*	Calculated molecular formula	Mass error (ppm)	Relevant MS/MS fragments (intensity)	Putative annotation
1		0.89	771.1971	$C_{33}H_{40}O_{21}$	−2.4	609 (3), 463 (8), 301 (100), 271 (8), 228 (3), 179 (5)	Quercetin-*O*-hexose-deoxyhexose-hexose
2		0.96	609.1449	$C_{27}H_{30}O_{16}$	−2	315 (100)	Rhamnetin/isorhamnetin-pentose-hexose or isomer
3		1.90	785.2131	$C_{34}H_{42}O_{21}$	−1.9	331 (89), 315 (100), 287 (51)	Unidentified mearnsetin-*O*-rhamninoside isomer
4	**UV_1**	2.15	755.2025	$C_{33}H_{40}O_{20}$	−2	609 (13), 447 (23), 301 (100), 255 (21), 192 (33)	Quercetin-*O*-deoxyhexose-hexose-deoxyhexose
5	**UV_2**	2.68	609.1452	$C_{27}H_{30}O_{16}$	−1,5	301 (100), 273 (5), 255 (34), 179 (7), 151 (29), 121 (3), 107 (3)	Quercetin-*O*-hexose-deoxyhexose
6		2.76	785.2124	$C_{34}H_{42}O_{21}$	−2.8	331 (100), 315 (27), 313 (59), 287 (8), 285 (24), 270 (5)	Mearnsetin-*O*-rhamninoside
7	**UV_3**	2.80	447.0920	$C_{21}H_{20}O_{11}$	−2.9	301 (100), 273 (42), 255 (69), 227 (30), 193 (34), 151 (51), 107 (14)	Quercetin-3-*O*-deoxyhexose
8	**UV_4**	3.11	769.2203	$C_{34}H_{42}O_{20}$	0.8	315 (82), 299 (100), 271 (34), 165 (14)	Rhamnetin-*O*-rhamninoside
9	**UV_5**	3.21	623.1603	$C_{28}H_{32}O_{16}$	−2.3	315 (28), 299 (100), 271 (33), 165 (4)	Rhamnetin-*O*-hexose-deoxyhexose
10		3.27	317.0296	$C_{15}H_{10}O_8$	−2.2	299 (58), 284 (100), 271 (62)	Myricetin
11		3.32	797.2130	$C_{35}H_{42}O_{21}$	−2	769 (7), 315 (97), 299 (100), 271 (19), 165 (16)	Glycosylated rhamnetin derivative
12	**UV_6**	3.39	783.2334	$C_{35}H_{44}O_{20}$	−2.5	329 (100), 313 (47), 299 (9), 271 (4), 165 (1)	Rhamnazin-rhamninoside
13		3.44	743.1450	$C_{34}H_{32}O_{19}$	−2	435 (100), 285 (58)	Unidentified flavonoid
14	**UV_7**	3.48	477.1028	$C_{22}H_{22}O_{12}$	−2.2	315 (19), 299 (100), 287 (6), 271 (92), 193 (1), 165 (7), 121 (1)	Rhamnetin-*O*-hexose
15	**UV_8**	3.70	623.1605	$C_{28}H_{32}O_{16}$	−2	461 (7), 315 (62), 299 (100), 271 (73), 193 (6), 165 (32)	Rhamnetin-*O*-deoxyhexose-hexose
16		3.79	447.0919	$C_{21}H_{20}O_{11}$	−3.1	315 (15), 299 (100), 271 (86), 165 (5)	Rhamnetin-*O*-pentose
17	**UV_9**	3.86	915.2561	$C_{43}H_{48}O_{22}$	−0.4	769 (30), 315 (100), 299 (48), 287 (1), 271 (9), 193 (3), 165 (13), 121 (2)	Rhamnetin-*O*-hexose-deoxyhexose-deoxyhexose-coumaroyl
18	**UV_{10}**	3.91	461.1079	$C_{22}H_{22}O_{11}$	−2.2	315 (24), 299 (100), 271 (88), 165 (13)	Rhamnetin-*O*-deoxyhexose
19	**UV_{11}**	4.04	915.2562	$C_{43}H_{48}O_{22}$	−0.3	769 (3), 315 (100), 299 (25), 287 (2), 271 (6), 193 (4), 165 (17), 121 (3)	Rhamnetin-*O*-hexose-deoxyhexose-deoxyhexose-coumaroyl
20	**UV_{12}**	4.32	915.2562	$C_{43}H_{48}O_{22}$	−0.3	769 (10), 315 (100), 299 (60), 287 (1), 271 (13), 193 (4), 165 (1), 121 (1)	Rhamnetin-*O*-hexose-deoxyhexose-deoxyhexose-coumaroyl
21	**UV_{13}**	4.56	401.0873	$C_{20}H_{18}O_9$	−1.3	269 (100), 241 (10), 225 (23), 197 (5)	Emodin-*O*-pentose
22		4.94	315.0466	$C_{16}H_{12}O_7$	−14	300 (40), 272 (25), 165 (100), 149 (19), 121 (73)	Rhamnetin
23	**UV_{14}**	5.18	313.0340	$C_{16}H_{10}O_7$	−4.4	298 (100), 269 (4), 254 (3), 226 (9), 213 (4), 197 (3)	Unidentified dihydroxy-methoxy-carboxy-anthraquinone
24	**UV_{15}**	5.24	415.1024	$C_{21}H_{20}O_9$	−2.5	269 (100), 241 (10), 225 (29), 213 (4), 197 (5)	Emodin-*O*-deoxyhexose
25	**UV_{16}**	6.39	269.0443	$C_{15}H_{10}O_5$	−4.6	241 (100), 225 (24), 213 (28), 210 (47), 197 (39), 195 (49)	Emodin

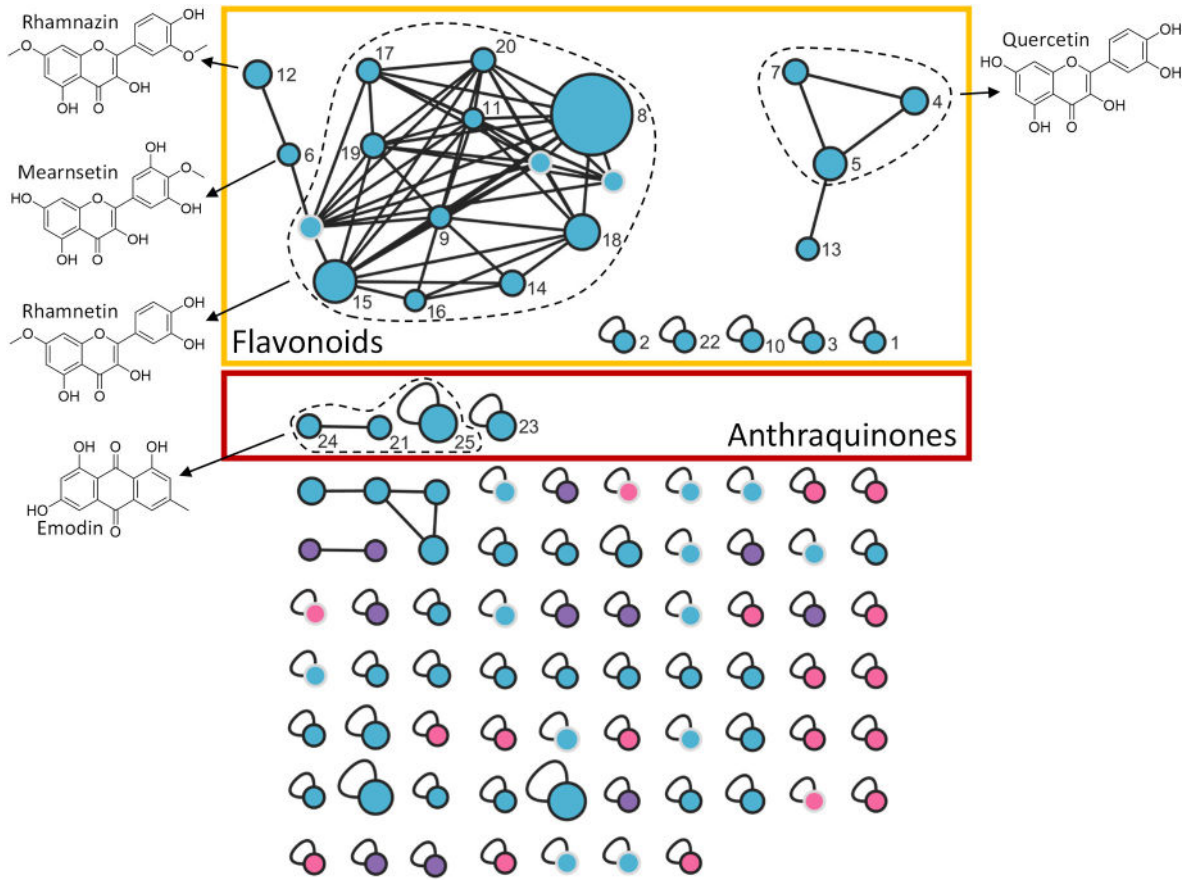

Fig. 4. Molecular network representation of the LC-MS dataset (after blanks filtering) obtained with extracts of aged (T_1: eq. 3 years, T_2: eq. 30 years, T_3: eq. 300 years) and unaged (T_0) fabrics dyed with berries of *R. cathartica*. Nodes are colored according to heatmap groups: Blue: Chemical markers of unaged or slightly faded fabrics (specific to T_0-T_1 conditions); Pink: Chemical markers of intermediary aged fabrics (specific to T_1 and T_2 conditions); Purple: Chemical markers of very or even completely faded fabrics (specific to T_2 and T_3 conditions). Compounds that were annotated are numbered (**1**–**25**) and *m/z* features that were not identified as molecular ions (i.e. fragments, adducts or isotopes) have a grey border. Lastly, colored frames highlight flavonoids (yellow) and anthraquinones (red) and the chemical structures of the main identified aglycones are displayed. (For interpretation of the references to color in this figure legend, the reader is referred to the Web version of this article.)

pattern between *m/z* features and can help identify compounds by annotation propagation. The molecular network was enriched using all the data gathered during the study. Nodes were colored according to the heatmap group attributed to each feature (unaged, intermediary or degradation markers) and their size was linked to the peak intensity in T_0 extracts. Annotated features were numbered and the structure of the main annotated aglycones were added. Lastly, colored frames were used to highlight flavonoids (yellow) and anthraquinones (red). A large cluster of methoxylated flavonoids, including rhamnazin, mearnsetin and rhamnetin derivatives was observed, as well as a smaller cluster containing mainly quercetin derivatives. Five features annotated as flavonoids (Compounds **1**–**3**, **10** and **22**) did not cluster with any other feature, which could potentially be attributed to their lower intensity, leading to less detected fragment ions in the MS/MS spectra. Three of the four detected anthraquinones were annotated as emodin and one glycosylated derivative (Compounds **21** and **24**) which were clustered together.

All glycosylated compounds displayed characteristic losses of *O*-pentose (132 u), *O*-deoxyhexose (146 u), *O*-hexose (162 u) or their combination. Stereoisomers of sugars cannot be differentiated by HRMS/MS [45]. Hence, in the putative identifications suggested here, the sugars were labelled as hexose, deoxyhexose or pentose. The only exception was rhamninoside (*L*-rhamnopyranosyl-(1 → 3)-*O*-*α*-*L*-rhamnopyranosyl-(1 → 6)-*O*-*β*-*D*-galactopyranoside) that was proposed for all deoxyhexose-deoxyhexose-hexose glycan parts in the absence of contrary information as this structural moiety is characteristic of extracts from *Rhamnus* spp. [46]. Complete fragmentation of annotated compounds and MS/MS spectra can be found in Supplementary Table S4.

3.2.2.1. Quercetin derivatives. Compounds **1**, **4**, **5** and **7** shared the same aglycone part, characterized by a fragment ion at *m/z* 301 ($[Y_0]^-$, $C_{15}H_9O_7^-$) and *m/z* 300 ($[Y_0–H]^{\bullet-}$, $C_{15}H_8O_7^{\bullet-}$). Diagnostic retrocyclization fragment ions of quercetin were observed in the MS/MS spectra of these four compounds at *m/z* 151 ($[^{1,2}A–CO]^-$), *m/z* 179 ($[^{1,2}A]^-$), *m/z* 121 ($[^{1,2}B]^-$), and/or *m/z* 107 ($[^{1,2}A–CO–CO_2]^-$) [47]. Thus, compounds **1**, **4**, **5** and **7** were putatively annotated as glycosylated derivatives of quercetin, a flavonoid commonly described in extracts of *R. cathartica* [46].

Compound **1** was characterized by a (-)-ESI-MS spectrum with a deprotonated quasi-molecular ion at *m/z* 771.1971, which corresponds to the molecular formula $C_{33}H_{40}O_{21}$. The MS/MS spectrum of **1** showed the presence of quercetin, yielded after the consecutive losses of one hexose unit (*m/z* 609.1400; $[Y_2]^-$), one deoxyhexose unit (*m/z* 463.0782; $[Y_1]^-$) and a second hexose unit (*m/z* 301.0362, $[Y_0]^-$). Thus, compound **1** was putatively annotated as quercetin-*O*-hexose-deoxyhexose-hexose, a compound that was never detected before in plants of the *Rhamnus* genus to our knowledge.

Compound **4**, also detected by LC-DAD as $\mathbf{UV_1}$, was characterized by a deprotonated quasi-molecular ion at *m/z* 755.2025, observed on its (-)-ESI-MS spectrum, which corresponded to the molecular formula $C_{33}H_{40}O_{20}$. Its MS/MS spectrum showed fragment ions at *m/z* 609.1486 ($[Y_2]^-$), *m/z* 447.0886 ($[Y_1]^-$) and *m/z* 301.0322 ($[Y_0]^-$) characteristic of

a quercetin aglycone part obtained after the consecutive losses of one deoxyhexose unit (146 u), one hexose unit (162 u), and a second deoxyhexose unit (146 u). This type of glycan sequence is not typical of the *Rhamnus* genus and does not correspond to a rhamninoside moiety. Thus, compound **4** was putatively annotated as quercetin-*O*-deoxyhexose-hexose-deoxyhexose.

The deprotonated quasi-molecular ion at *m/z* 609.1452 observed on the (-)-ESI-MS spectrum of compound **5** (also detected by LC-DAD as **UV$_2$**) was consistent with a molecular formula of $C_{27}H_{30}O_{16}$. The MS/MS spectrum of **5** showed a quercetin aglycone part (*m/z* 301.0328, $[Y_0]^-$) yielded after the loss of a diglycoside (308 u) containing one deoxyhexose unit and one hexose unit. The absence of $[Y_1]^-$, $[Y_1–H]^{\bullet-}$ and $[Y_0–2H]^{\bullet-}$ fragment ions indicated a *O*-diglycoside rather than a di-*O*-glycoside [45]. Compound **5** was thus putatively annotated as quercetin-*O*-hexose-deoxyhexose, a glycosylated flavonoid previously described in *R. cathartica* [48] and several other *Rhamnus* species [49–51].

Compound **7** (also detected by LC-DAD as **UV$_3$**) showed on its (-)-ESI-MS spectrum a deprotonated quasi-molecular ion at *m/z* 447.0920 corresponding to the molecular formula $C_{21}H_{20}O_{11}$. This ion and the fragment ion observed at *m/z* 301.0318, ($[Y_0]^-$) were typical of the presence of a quercetin aglycone part obtained after the loss of one deoxyhexose unit (146 u). Thus, compound 7 was putatively annotated as quercetin-*O*-deoxyhexose. This glycosylated flavonoid has been previously described in *R. cathartica* [52,53] as well as in other *Rhamnus* spp [28,51].

3.2.2.2. Rhamnetin derivatives. Compounds **8**, **9**, **11** and **14**–**20** all shared the same aglycone part which was characterized by the presence of typical ion fragments at *m/z* 315 ($[Y_0]^-$, $C_{16}H_{11}O_7^-$) and *m/z* 314 ($[Y_0–H]^{\bullet-}$, $C_{16}H_{10}O_7^{\bullet-}$) on their MS/MS spectra. The (-)-ESI-MS spectrum analysis of compound **22** showed a deprotonated quasi-molecular ion at *m/z* 315.0466 ($[M - H]^-$) consistent with a molecular formula of $C_{16}H_{12}O_7$, which corresponds precisely to this aglycone. Characteristic fragment ions corresponding to the successive loss of a methyl group ($[Y_0–CH_3]^{\bullet-}$, *m/z* 300 or $[Y_0–CH_4]^-$, *m/z* 299) and a carbonyl group (-CO, 28 u) were observed on the MS/MS spectrum of these compounds [54]. Moreover, several retrocyclization fragment ions were also detected at *m/z* 165 ($^{1,3}A^-$) and *m/z* 121 ($^{0,4}A^-$) [28]. These data were consistent with the putative annotation of **22** as rhamnetin, a flavonoid already described in extracts of *R. cathartica* [28,41]. Compounds **8**, **9**, **11** and **14**–**20** were then annotated as glycosylated derivatives of rhamnetin.

The deprotonated quasi-molecular ion at *m/z* 769.2203 observed on the (-)-ESI-MS spectrum of compound **8** (also detected by LC-DAD as **UV$_4$**) corresponded to the molecular formula $C_{21}H_{20}O_{11}$. Its MS/MS spectrum showed a fragment ion at *m/z* 315.0453 ($[Y_0]^-$), which corresponds to rhamnetin obtained after the loss of one hexose unit and two deoxyhexose units without any intermediary ion fragments. Compound **8** was putatively identified as rhamnetin-*O*-rhamninoside, a flavonoid previously described in *R. cathartica* [46].

The (-)-ESI-MS spectrum of compound **9**, a flavonoid also detected by LC-DAD as **UV$_5$** showed a deprotonated quasi-molecular ion at *m/z* 623.1603 ($C_{28}H_{32}O_{16}$). From this parent ion, a fragment ion (*m/z* 315.0473 $[Y_0]^-$) was observed on the MS/MS spectrum, corresponding to rhamnetin obtained after the loss of one deoxyhexose unit (146 u) and one hexose unit (162 u). The absence of $[Y_1]^-$, $[Y_1–H]^{\bullet-}$ fragment ions indicated a probable rhamnetin-*O*-diglycoside rather than a di-*O*-glycoside [45]. Thus, compound **9** was putatively annotated as rhamnetin-*O*-hexose-deoxyhexose, a compound previously described in *R. cathartica* [28]. The LC-DAD data presented earlier led to the hypothesis that compound **9** (**UV$_5$**) could be a degradation product. This putative annotation supports this hypothesis and shows that compound **9** could be obtained from the main dye of the extract, compound **8** (**UV$_4$**), after the loss of a deoxyhexose.

Compound **11** showed on its (-)-ESI-MS spectrum a deprotonated quasi-molecular ion at *m/z* 797.2131, corresponding to the proposed formula $C_{35}H_{42}O_{21}$. Its fragmentation MS/MS spectra displayed a fragment ion observed at *m/z* 315.0480 ($[Y_0]^-$) corresponding to rhamnetin obtained after the consecutive losses of a –CO group (*m/z* 769.2184), and of a triglycoside containing one hexose unit and two deoxyhexose units (454 u). The chemical structure of compound **11** was not further elucidated.

Compound **14** (also detected by LC-DAD as **UV$_7$**) was characterized by a deprotonated quasi-molecular ion at *m/z* 477.1028 ($C_{22}H_{22}O_{12}$). The corresponding MS/MS spectrum showed an ion fragment at *m/z* 315.0480 ($[Y_0]^-$) which can be attributed to a rhamnetin moiety obtained after the loss of one hexose unit (162 u). Compound **14** was putatively annotated as rhamnetin-*O*-hexose; a compound which has not been described before in plants of the genus *Rhamnus*.

A deprotonated quasi-molecular ion at *m/z* 623.1605 ($C_{28}H_{32}O_{16}$) was observed on the (-)-ESI-MS spectrum of compound **15**, a flavonoid also detected by LC-DAD as **UV$_8$**. The MS/MS spectrum showed two characteristic ion fragments at *m/z* 461.0884 ($[Y_1]^-$) and *m/z* 315.0520 ($[Y_0]^-$) corresponding to a rhamnetin obtained after the consecutive losses of one hexose unit (162 u) and one deoxyhexose unit (146 u). Due to the high $[Y_0]^-/[Y_1]^-$ ratio, the prominence of $[Y_0–H]^{\bullet-}$ and the absence of $[Y_1–H]^{\bullet-}$ and $[Y_0–2H]^{\bullet-}$, compound **15** was hypothesized an *O*-diglycoside rather than a di-*O*-glycoside [45]. Thus, compound **15** was putatively annotated as rhamnetin-*O*-deoxyhexose-hexose, a glycosylated flavonoid previously observed in several *Rhamnus* species [28,48].

The (-)-ESI-MS spectrum of compound **16** showed a deprotonated quasi-molecular ion at *m/z* 447.0919, consistent with the molecular formula $C_{21}H_{20}O_{11}$. The resulting MS/MS fragmentation of this parent ion gave an ion at *m/z* 315.0474 ($[Y_0]^-$) corresponding to a rhamnetin moiety obtained after the loss of a pentose (132 u). Thus, compound **16** was putatively annotated as rhamnetin-*O*-pentose, which, to our knowledge, has not been previously described in the *Rhamnus* genus.

The same deprotonated quasi-molecular ion at *m/z* 915.256 ($C_{43}H_{48}O_{22}$) was observed on the (-)-ESI-MS spectra of compounds **17**, **19** and **20**, also detected by LC-DAD as **UV$_9$**, **UV$_{11}$** and **UV$_{12}$**. All three shared a common MS/MS fragmentation pattern with the loss of a coumaroyl (146 u) leading to a fragment ion at *m/z* 769.22 ($C_{34}H_{42}O_{20}$) and then the direct loss of a triglycoside (454 u) containing one hexose unit and two deoxyhexose units, yielding rhamnetin (*m/z* 315.05, $[Y_0]^-$). Considering their different retention times (from 3.86 to 4.32 min), compounds **17**, **19** and **20** were putatively annotated as isomers of rhamnetin-*O*-hexose-deoxyhexose-deoxyhexose-coumaroyl. Such a chemical structure has been previously described in *Rhamnus petiolaris* [55].

Compound **18**, also detected by LC-DAD as **UV$_{10}$**, was characterized by a deprotonated quasi-molecular ion at *m/z* 461.1079 corresponding to the molecular formula $C_{22}H_{22}O_{11}$. The fragment ion at *m/z* 315.467 ($[Y_0]^-$) observed on its (-)-ESI-MS/MS spectrum was consistent with a rhamnetin aglycone obtained after the loss of one deoxyhexose unit (146 u). Thus, compound **18** was putatively identified as rhamnetin-*O*-deoxyhexose, a glycosylated flavonoid previously described in extracts of *R. cathartica* [48,52].

3.2.2.3. Other flavonoids. Compound **2** was characterized by a deprotonated quasi-molecular ion observed at *m/z* 609.1449 ($C_{27}H_{30}O_{16}$) on its (-)-ESI-MS spectrum. The corresponding MS/MS data showed the loss of a diglycoside containing one pentose unit (132 u) and one hexose unit (162 u), leading to a fragment ion at *m/z* 315.0424 (Y_0^-) characteristic of a rhamnetin or an isorhamnetin aglycone part. No characteristic retrocyclization ion fragments from rhamnetin (*m/z* 165 and 121) or isorhamnetin (*m/z* 151 and 107) nor $[Y_0–CH_3]^{\bullet-}$ (*m/z* 300), a fragment previously described as dominant in the MS/MS fragmentation spectrum of isorhamnetin, were observed [28,54]. Thus, compound **2** was annotated as a rhamnetin/isorhamnetin-pentose-hexose or isomer.

The (-)-ESI-MS spectrum of compound **12**, also detected by LC-DAD

as **UV_6**, showed a deprotonated quasi-molecular ion at *m/z* 783.2334 ($C_{35}H_{44}O_{20}$). The corresponding MS/MS data showed a fragment ion corresponding to the loss of a diglycoside (454 u) containing one hexose unit and two deoxyhexose units, which led to the fragment ion of the aglycone part (*m/z* 329.0645, $C_{17}H_{14}O_7$). The MS/MS spectra of compound **12** also showed fragments ions annotated as $[Y_0–CH_3]^{\bullet-}$ (*m/z* 314.0405), $[Y_0–2CH_3]^-$ (*m/z* 299.0174), $[Y_0–2CH_3–CO]^-$ (*m/z* 271.0222) and $^{1,3}A^-$ (*m/z* 165.0150). This MS/MS fragmentation pattern indicated two methoxy groups positioned on the A ring and on the B ring, respectively [28]. From these results, compound **12** was putatively annotated as rhamnazin-rhamninoside, a compound previously described in *R. cathartica* [46].

Compounds **3** and **6** are two isomers characterized by the presence of a deprotonated quasi-molecular ion on their respective (-)-ESI-MS spectra at *m/z* 785.21, which corresponded to the molecular formula $C_{34}H_{42}O_{21}$. Both MS/MS fragmentation patterns displayed the direct loss of a triglycoside (454 u) containing one hexose unit and two deoxyhexose units, which led to fragment ions detected at *m/z* 331.0452 and 331.0476 for **3** and **6**, respectively. The calculated molecular formula for both aglycone parts was $C_{16}H_{12}O_8$. However, differences observed on their MS/MS spectra indicated that the aglycones of compounds **3** and **6** had different chemical structures. It should be noted that on the molecular network, compound **6** was part of a cluster comprising mainly rhamnetin-type derivatives. More precisely, it was connected to the feature **MS_{482}** (*m/z* 769.2179, $C_{34}H_{42}O_{20}$) (Supplementary Table S3), a fragment of compound **11** annotated as rhamnetin-*O*-hexose-deoxyhexose-deoxyhexose, as well as to compound **12** (*m/z* 783.2334, $C_{35}H_{44}O_{20}$), which was annotated as rhamnazin-*O*-hexose-deoxyhexose-deoxyhexose. The mass differences between these compounds indicated that the aglycone of compound **6** could be a hydroxylated rhamnetin derivative, such as mearnsetin, a flavonoid previously described in *Rhamnus pallasii* [56]. Thus, compound **6** was putatively annotated as mearnsetin-*O*-rhamninoside. Compound **3** was not included in a molecular network cluster and apart from the consecutive losses of a CH_4 (*m/z* 315.0094) and a CO (*m/z* 287.0198), its MS/MS fragmentation pattern was different from compound **6**. Thus, compound **3** remained unidentified.

A deprotonated quasi-molecular ion was observed at *m/z* 317.0296 ($C_{15}H_{10}O_8$) on the (-)-ESI-MS spectrum of compound **10**. Three fragment ions corresponding to the loss of H_2O, followed by either the loss of CH_3 or CO were detected at *m/z* 299.0152 ($C_{15}H_8O_7$), 283.9944 ($C_{14}H_5O_7$) and 271.0241 ($C_{14}H_8O_6$) in its MS/MS spectrum. The CANOPUS tool on Sirius classified compound **10** as a flavonoid. However, its MS/MS fragmentation pattern indicated an *O*-methylated compound as well as multiple CO losses (28 u) that did not correspond to any $C_{15}H_{10}O_8$ flavonoid. Thus, compound **10** remained unidentified. However, its additional two H-atoms (compared to rhamnetin) could point to a 2,3-dihydroflavonol, which is consistent with the observation of a H_2O loss with concomitant formation of a flavone fragment.

Compound **13** was characterized by a deprotonated quasi-molecular ion at *m/z* 743.1450, which corresponded to the molecular formula $C_{34}H_{32}O_{19}$. The loss of a diglycoside containing one deoxyhexose unit and one hexose unit was detected at *m/z* 435.0331 ($C_{22}H_{12}O_{10}$). Furthermore, another main fragment ion was detected at *m/z* 285.0015 ($C_{14}H_6O_7$). Compound **13** was classified as a flavonoid using CANOPUS on Sirius and was connected to compound **5** (quercetin-*O*-deoxyhexose-hexose) in the quercetin cluster of the molecular network. However, no flavonoid corresponding to this fragmentation pattern was found and compound **13** remained unidentified.

3.2.2.4. Anthraquinones. Compounds **21** and **23**–**25**, already detected by LC-DAD at 450 nm as **UV_{13}**-**UV_{16}**, were thus putatively annotated as anthraquinones. Compounds **21** and **24** were glycosylated forms of the same aglycone, characterized by a fragment ion at *m/z* 269.0439 and *m/z* 269.0438 ($C_{15}H_{10}O_5$), which corresponded to compound **25**. The common MS/MS fragmentation pattern observed on their respective (-)-ESI-MS/MS spectra confirmed that **21** and **24** were glycosylated forms of **25**.

Compound **25** (**UV_{16}**) was characterized by a deprotonated quasi-molecular ion at *m/z* 269.0443 ($C_{15}H_{10}O_5$) observed on its (-)-ESI-MS spectrum. Characteristic losses of CO (*m/z* 241.0494), CO_2 (*m/z* 225.0531) and their combination (*m/z* 197.0580) were detected, as well as other fragment described in the fragmentation pattern of emodin such as *m/z* 210.0316, 182.0355 and 171.0424 [28]. Compound **25** was then putatively annotated as emodin, an anthraquinone already described in *R. cathartica* [28,41] and in other *Rhamnus* species [57].

The deprotonated quasi-molecular ions at *m/z* 401.0873 and *m/z* 415.1024 on the (-)-ESI-MS spectrum of compound **21** (**UV_{13}**) and compound **24** (**UV_{15}**), corresponded to the molecular formulae $C_{20}H_{18}O_9$ and $C_{21}H_{20}O_9$, respectively. Their MS/MS data showed the neutral loss of one pentose unit (132 u) for **21** and of one deoxyhexose unit (146 u) for **24**, leading to the aglycone. Thus, compound **21** was putatively annotated as emodin-*O*-pentose and compound **24** as emodin-*O*-deoxyhexose. Both these compounds have already been described in the bark of *Rhamnus frangula* as frangulins B and A, respectively [58]. Emodin-deoxyhexose has also been identified in the bark of *R. cathartica* [59] as well as in berries of *Rhamnus ussuriensis* [51], meaning its presence in *R. cathartica* berries is plausible.

Compound **23** (**UV_{14}**) was characterized by a deprotonated quasi-molecular ion at *m/z* 313.0340 ($C_{16}H_{10}O_7$). The main fragment ion observed on its (-)-ESI-MS/MS spectrum (at *m/z* 298.0098) corresponded to the loss of a CH_3 group, which can be observed in *O*-methylated anthraquinones. Another fragment ion observed at *m/z* 269.0431 ($[M\text{-}H\text{-}CO_2]^-$) corresponded to the loss of carboxylic acid. Moreover, the loss of CO was observed in multiple fragments. This MS/MS fragmentation pattern is in good correlation with the literature for an anthraquinone with a methoxy and a carboxylic acid group [60,61]. According to its chemical formula, compound **23** would also be substituted with 2 hydroxyl groups, but their losses were not detected in the MS/MS spectra. Compound **23** was thus annotated as a dihydroxy-methoxy-carboxy-anthraquinone. To our knowledge, no such compound has been previously described in Rhamnaceae.

3.2.3. Molecular networking

The molecular network was not only used as an annotation tool, but also to visualize the global chemical composition of aged and unaged extracts. To that end, the molecular network was enriched using the data obtained in the previous parts of this manuscript (Fig. 4). The node sizes were correlated to the mean T_0 peak area measured on the LC-MS base peak chromatograms (BPC) and each node was colored depending on the groups previously defined with the heatmap (unaged, intermediary or degradation markers). Moreover, the annotation IDs and the chemical structures of some aglycone flavonoids and anthraquinones were added (Fig. 4). A molecular network labelled with the feature list identifiers is also available in Supplementary Fig. S3.

Three clusters of four or more compounds were observed on the molecular network. The largest one corresponded mostly to rhamnetin derivatives (compounds **8**, **9**, **11** and **14**–**20**), as well as glycosylated forms of mearnsetin (compound **6**) and rhamnazin (compound **12**), which have all been described in extracts of *Rhamnus* species [28,46,56]. Another cluster corresponded to quercetin derivatives (compounds **4**, **5** and **7**), which are flavonoids found in many plants and also commonly described in extracts of *Rhamnus* species [46]. Other flavonoids (compounds **1**–**3**, **10**, and **22**), still annotated as rhamnetin or quercetin derivatives, were not included in clusters. Interestingly, kaempferol was not detected. However, it is a well described compound of the *Rhamnus* genus that has been proposed as a diagnostic compound to differentiate *R. cathartica* from other species of this same genus [46]. We hypothesized that it was either not fixed on the fabrics during dyeing or not recovered during extraction.

Four anthraquinones (compounds **21** and **23**–**25**) were annotated,

three of them being emodin and its glycosylated derivatives. All annotated anthraquinones were also previously observed by LC-DAD, but almost half of the annotated flavonoids were not. This illustrates the higher sensitivity of LC-MS compared to LC-DAD. All flavonoids and anthraquinones were classified as unaged markers, which shows that the degradation was too rapid to observe intermediary degradation products, such as those formed through the hydrolysis of glycosidic bonds. It has been proven that degradation of flavonoids and anthraquinones leads to the formation of degradation products that no longer absorb light in the visible region, notably hydroxybenzoic and hydroxyphenylacetic acids [1,7]. These compounds, as well as other degradation markers and light-induced degradation products of flavonoids described in the literature (e.g., depsides and chalcones) were specifically searched in all samples, but were either not detected at all, or as traces that could not be annotated robustly due to a lack of MS/MS fragmentation data. This suggested that the accelerated ageing treatment directly caused the full degradation of these dye compounds into more volatile compounds, which is most likely due to the chosen ageing parameters. Indeed, high levels of ventilation and a temperature up to 60 °C for the longest ageing treatment were applied. Moreover, this work was conducted on fabric mordanted with alum, which has been described to affect the ageing of the fixed dye compounds [62].

3.3. What remains in faded fabrics? Assessment of the remaining dyes

The specific flavonoid and anthraquinone contents of a dye extract can help determine which plant has been used to dye a historical fabric [48]. However, in less preserved fabrics, when the color has been lost over the years, the detection and identification of dye traces can be difficult [1]. In those cases, LC-MS based metabolomics should be considered. Indeed, in this study, the LC-MS based approach enabled the detection of twice as many flavonoids as the LC-DAD approach. Moreover, almost all detected flavonoids and anthraquinones were putatively identified without any standard.

The focus was put on the light-bleached T_3 samples. The color in these samples was detectable neither by human eye, nor by using CIELAB colorimetry and only the main dye could still be detected using LC-DAD. The features list showed that most dye compounds -including anthraquinones-were still detected in T_3 extracts using LC-MS. Two Venn diagrams (Fig. 5) were constructed to illustrate the differences between the two methods (LC-DAD *vs* LC-MS) and further study what remains when the color is gone. The diagrams were based on the peak intensity in LC-DAD at 350 nm for flavonoids and 450 nm for anthraquinones (Fig. 5A) and LC-MS (Fig. 5B) of the 16 compounds detected in LC-DAD. The Venn diagram was annotated to display the putative identification of detected compounds.

Fig. 5A showed that, as previously determined, the four anthraquinones (**UV_{13}** to **UV_{16}**) were only detected in T_0 using LC-DAD. Also, only three flavonoids were above the LOD in T_2 samples and none in T_3 samples. On the contrary, according to Fig. 5B and as stated before, LC-MS enabled the detection of all flavonoids and anthraquinones in T_2 extracts and of more than half of them were still detected in T_3 extracts. This showed the sensitivity of the method as both flavonols and anthraquinones were detected, even in low concentrations, in aged extracts.

A third Venn diagram was made using the LC-MS data, this time including all flavonoids and anthraquinones (Supplementary Fig. S4). The nine flavonoids that were not detected at all using LC-DAD were only detected until T_2, which is probably due to their lower concentration.

The dye compounds that remained in T_3 extracts were annotated as seven flavonoids, including a quercetin-diglycoside, a rhamnazin-triglycoside and five glycosylated derivatives of rhamnetin, as well as three anthraquinones, including emodin and emodin-pentose. These results show the great potential of this approach in the study of ancient fabrics, even after the loss of all visible colors. Indeed, taken separately, these molecules are not specific to the *Rhamnus* genus. However, the simultaneous detection of emodin, rhamnetin, rhamnazin and quercetin, as well as multiple triglycosylated flavonoids (mainly rhamninoside) is very specific of the *Rhamnus* genus [48–50]. Thus such composition in an extract from a historical fabric would have most likely led to the hypothesis that a plant from the *Rhamnus* genus had been used to dye it.

4. Conclusion

This study focused on the evolution of color and chemical composition of extracts obtained from cotton fabrics dyed with *R. cathartica* berries after light-induced accelerated ageing. The color fading was gradual and led to degraded samples lighter than the undyed cotton fabrics where dyes could not be detected by LC-DAD. LC-MS based metabolomics revealed a full picture of the dye composition in all extracts. Moreover, about two thirds of the 25 annotated dye compounds were still detected in the fully degraded samples (T_3). Then, the original dye could be found even in white-appearing fabrics.

Thus, future works should focus on dye compounds using targeted metabolomics, which would prove even more sensitive. Working with different fabrics, such as wool or silk, and multiplying the mordants and dye plants would thus yield different chemical markers and deepen our interpretations. Moreover, working with a softer ageing process in terms of temperature and duration could potentially enable the detection of

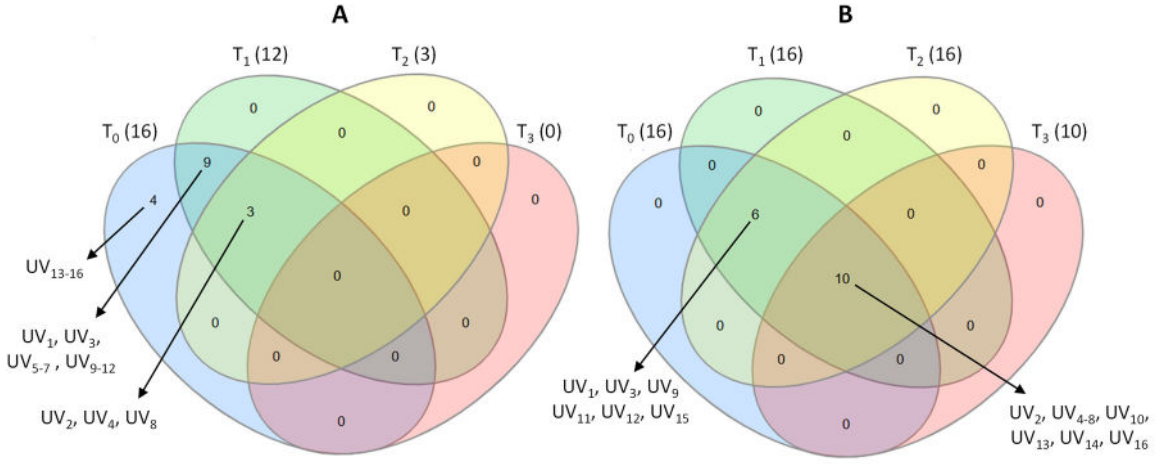

Fig. 5. Venn diagrams showing the detection of the compounds **UV_1.UV_{16}** by (**A**) LC-DAD and (**B**) LC-MS in the extracts obtained from aged (T_1: eq. 3 years, T_2: eq. 30 years, T_3: eq. 300 years) and unaged (T_0) fabrics dyed with *R. cathartica* berries. The number of detected compounds in each group is showed in parenthesis.

specific intermediary or degradation chemical markers that were not observed in this study.

CRediT authorship contribution statement

Marine Chambaud: Writing – original draft, Visualization, Validation, Investigation, Formal analysis, Data curation. **Lindsay Mas-Normand:** Writing – review & editing, Validation, Methodology, Investigation. **Céline Joliot:** Resources, Investigation. **Carole Mathe:** Writing – review & editing, Supervision, Funding acquisition, Conceptualization. **Olivier Dangles:** Writing – review & editing, Supervision, Funding acquisition, Conceptualization. **Gérald Culioli:** Writing – review & editing, Visualization, Supervision, Resources, Project administration, Methodology, Funding acquisition, Data curation, Conceptualization.

Funding sources

The PhD grant of L. Mas-Normand was financially supported by the IMPLANTEUS "Sustainable Mediterranean Agriculture for Health" Graduate School of Avignon University funded from the French National Research Agency as part of the France 2023 investment program for the future, under reference ANR-18-EURE-0009. One part of the LC-MS analyses was granted by the TERSYS federative research structure (Avignon University, France).

Declaration of competing interest

The authors declare that they have no known competing financial interests or personal relationships that could have appeared to influence the work reported in this paper.

Acknowledgements

The authors are grateful to Dr. R. Lugan, V. Kuentz, and S. Raynal for their help during the acquisition of LC-MS profiles on the "Metaboscope" platform (Avignon University, France), to Z. Moubtassim (IMBE, Avignon University, France) for her help with extraction and sample preparation and to Dr. E. Garayev (IMBE, Aix-Marseille University, France) for the script used to correct the *m/z* values of precursor ions of MS/MS scans.

Appendix A. Supplementary data

Supplementary data to this article can be found online at https://doi.org/10.1016/j.dyepig.2026.113625.

Data availability

The following sentence has been added to the Ms: Raw data for LC-(-)-ESI-HRMS/MS analyses were deposited on the MassIVE platform under the ID MSV000100116.

References

[1] Colombini MP, Andreotti A, Baraldi C, Degano I, Łucejko JJ. Colour fading in textiles: a model study on the decomposition of natural dyes. Microchem J 2007; 85:174–82. https://doi.org/10.1016/j.microc.2006.04.002.
[2] Domínguez-Castillo C, Jiménez-Hidalgo M, López-Gámez J, Rodríguez-Hortal A, Alzaga-García M, Gallardo-Abárzuza M, et al. High-resolution mass spectrometry identification of dye compounds and their degradation products in American cochineal from a historic shipping cargo. Dyes Pigments 2023;216:111313. https://doi.org/10.1016/j.dyepig.2023.111313.
[3] Zhou X, Guo Y, Zhang H, Zhang L, Wu M, Zhang W. Shedding light on the composition and fading mechanisms of dye molecules in *Phellodendron amurense Rupr.* Dyed silk. J Photochem Photobiol Chem 2024;451:115496. https://doi.org/10.1016/j.jphotochem.2024.115496.
[4] Lech K. Analysing reds in Coptic textiles: insights from mass spectrometry. J Cult Herit 2025;71:274–81. https://doi.org/10.1016/j.culher.2024.12.007.
[5] Ahn C, Zeng X, Li L, Obendorf SK. Thermal degradation of natural dyes and their analysis using HPLC-DAD-MS. Fashion and Textiles 2014;1:22. https://doi.org/10.1186/s40691-014-0022-5.
[6] Analytical Methods Committee, Amctb No. 119. Microfade testing in cultural heritage. Anal Methods 2025:7570–3. https://doi.org/10.1039/D5AY90120K.
[7] Sharif S, Nabais P, Melo MJ, Pina F, Oliveira MC. Photoreactivity and stability of flavonoid yellows used in cultural heritage. Dyes Pigments 2022;199:110051. https://doi.org/10.1016/j.dyepig.2021.110051.
[8] Ferreira E., Quye A., McNab H., Hulme A. Photo-oxidation products of quercetin and morin as markers for the characterisation of natural yellow dyes in ancient textiles. In: Kirby J., editor. Dyes in history and archaeology-Vol. 18,London: Archetype; 2002,p. 63–72.
[9] Hendriks L, Martinent R, Spack C, Bourgnon G, Jucker AW, Portmann C. Identification of brazilein type B as a key marker for the presence of brazilwood in colored historical objects. Anal Methods 2025;17:7140–7. https://doi.org/10.1039/D5AY00798D.
[10] Witkowski B, Stachurska M, Lustyk P, Gierczak T, Biesaga M. Pitfalls of dye identification in historical fabrics. J Cult Herit 2025;72:180–90. https://doi.org/10.1016/j.culher.2025.02.003.
[11] Benli H, Bahtiyari M. Providing UV protection features for woolen fabric using buckthorn dye. J Nat Fibers 2023;20:2143978. https://doi.org/10.1080/15440478.2022.2143978.
[12] Fiehn O. Metabolomics – the link between genotypes and phenotypes. Plant Mol Biol 2002;48:155–71. https://doi.org/10.1023/A:1013713905833.
[13] Badillo-Sanchez D, Serrano Ruber M, Davies-Barrett A, Jones DJL, Hansen M, Inskip S. Metabolomics in archaeological science: a review of their advances and present requirements. Sci Adv 2023;9:eadh0485. https://doi.org/10.1126/sciadv.adh0485.
[14] Brownstein KJ, Tushingham S, Damitio WJ, Nguyen T, Gang DR. An ancient residue metabolomics-based method to distinguish use of closely related plant species in ancient pipes. Front Mol Biosci 2020;7:133. https://doi.org/10.3389/fmolb.2020.00133.
[15] Zimmermann M, Brownstein KJ, Pantoja Díaz L, Ancona Aragón I, Hutson S, Kidder B, et al. Metabolomics-based analysis of miniature flask contents identifies tobacco mixture use among the ancient Maya. Sci Rep 2021;11:1590. https://doi.org/10.1038/s41598-021-81158-y.
[16] Mas-Normand L, Dangles O, Mathe C, Culioli G. Identification of yellow dye plant chemical markers for applications in cultural heritage using LC-MS-based metabolomics and molecular networking. Microchem J 2025;218:115621. https://doi.org/10.1016/j.microc.2025.115621.
[17] Ji Y, Zhang R, Bensalel J, Morcol T, Gu R, Gallego-Delgado J, et al. Metabolomic and chemometric analyses of St. John's wort and related Asian *Hypericum* species linked to bioactivity. J Ethnopharmacol 2024;329:118163. https://doi.org/10.1016/j.jep.2024.118163.
[18] Ren C, Chen C, Dong S, Wang R, Xian B, Liu T, et al. Integrated metabolomics and transcriptome analysis on flavonoid biosynthesis in flowers of safflower (*Carthamus tinctorius* L.) during colour-transition. PeerJ 2022;10:e13591. https://doi.org/10.7717/peerj.13591.
[19] Christenhusz MJM, Byng JW. The number of known plants species in the world and its annual increase. Phytotaxa 2016;261:201–17. https://doi.org/10.11646/phytotaxa.261.3.1.
[20] Abu-Ghosh S, Sukenik N, Amar Z, Iluz D. Yellow dyes in archaeological textiles: sources, locations, identification, and challenges. J Archaeol Sci: Reports 2023;49: 104030. https://doi.org/10.1016/j.jasrep.2023.104030.
[21] Hofmann-de Keijzer R, de Keijzer M. *Plantae tinctoriae*: the 1759 dissertation on dye plants by Engelbert Jörlin. Heritage 2023;6:1502–30. https://doi.org/10.3390/heritage6020081.
[22] Cardon D. Le monde des teintures naturelles. Paris: Belin. 2014.
[23] Hagan E, Poulin J. The effect of prior exposure on the lightfastness of early synthetic dyes on textiles. Herit Sci 2022;10:138. https://doi.org/10.1186/s40494-022-00767-6.
[24] Sharif S, Nabais P, Melo MJ, Oliveira MC. Traditional yellow dyes used in the 21st century in central Iran: the knowledge of master dyers revealed by HPLC-DAD and UHPLC-HRMS/MS. Molecules 2020;25:908. https://doi.org/10.3390/molecules25040908.
[25] Marquet M. Guide des teintures naturelles. Plantes à fleurs. Paris: Belin; 2011.
[26] ISO/CIE 11664-4:2019(E) International standard.. Colorimetry — Part 4: CIE 1976 L*a*b* colour space. 2019.
[27] Zhang L, Tian K, Wang Y, Zou J, Du Z. Characterization of ancient Chinese textiles by ultra-high performance liquid chromatography/quadrupole-time of flight mass spectrometry. Int J Mass Spectrom 2017;421:61–70. https://doi.org/10.1016/j.ijms.2017.04.009.
[28] Lech K. Universal analytical method for characterization of yellow and related natural dyes in liturgical vestments from Krakow. J Cult Herit 2020;46:108–18. https://doi.org/10.1016/j.culher.2020.04.011.
[29] Heberle H, Meirelles GV, Da Silva FR, Telles GP, Minghim R. InteractiVenn: a web-based tool for the analysis of sets through Venn diagrams. BMC Bioinf 2015;16: 169. https://doi.org/10.1186/s12859-015-0611-3.
[30] Chambers MC, Maclean B, Burke R, Amodei D, Ruderman DL, Neumann S, et al. A cross-platform toolkit for mass spectrometry and proteomics. Nat Biotechnol 2012;30:918–20. https://doi.org/10.1038/nbt.2377.
[31] Breaud C, Lallemand L, Mares G, Mabrouki F, Bertolotti M, Simmler C, et al. LC-MS based phytochemical profiling towards the identification of antioxidant markers in some endemic *Aloe* species from Mascarene Islands. Antioxidants 2023;12:50. https://doi.org/10.3390/antiox12010050.

[32] Schmid R, Heuckeroth S, Korf A, Smirnov A, Myers O, Dyrlund TS, et al. Integrative analysis of multimodal mass spectrometry data in MZmine 3. Nat Biotechnol 2023; 41:447–9. https://doi.org/10.1038/s41587-023-01690-2.
[33] Pang Z, Lu Y, Zhou G, Hui F, Xu L, Viau C, et al. MetaboAnalyst 6.0: towards a unified platform for metabolomics data processing, analysis and interpretation. Nucleic Acids Res 2024;52:W398–406. https://doi.org/10.1093/nar/gkae253.
[34] Wang M, Carver JJ, Phelan VV, Sanchez LM, Garg N, Peng Y, et al. Sharing and community curation of mass spectrometry data with Global Natural Products Social Molecular Networking. Nat Biotechnol 2016;34:828–37. https://doi.org/10.1038/nbt.3597.
[35] Shannon P, Markiel A, Ozier O, Baliga NS, Wang JT, Ramage D, et al. Cytoscape: a software environment for integrated models of biomolecular interaction networks. Genome Res 2003;13:2498–504. https://doi.org/10.1101/gr.1239303.
[36] Dührkop K, Nothias L-F, Fleischauer M, Reher R, Ludwig M, Hoffmann MA, et al. Systematic classification of unknown metabolites using high-resolution fragmentation mass spectra. Nat Biotechnol 2021;39:462–71. https://doi.org/10.1038/s41587-020-0740-8.
[37] Dührkop K, Fleischauer M, Ludwig M, Aksenov AA, Melnik AV, Meusel M, et al. Sirius 4: a rapid tool for turning tandem mass spectra into metabolite structure information. Nat Methods 2019;16:299–302. https://doi.org/10.1038/s41592-019-0344-8.
[38] Schrimpe-Rutledge AC, Codreanu SG, Sherrod SD, McLean JA. Untargeted metabolomics strategies—challenges and emerging directions. J Am Soc Mass Spectrom 2016;27:1897–905. https://doi.org/10.1007/s13361-016-1469-y.
[39] Durmus D. CIELAB color space boundaries under theoretical spectra and 99 test color samples. Color Res Appl 2020;45:796–802. https://doi.org/10.1002/col.22521.
[40] Michalski S. Agent of deterioration: light, ultraviolet and infrared. Canadian Conservation Institute; 2018. https://www.canada.ca/en/conservation-institute/services/agents-deterioration/light.html. [Accessed 5 June 2025].
[41] Deveoglu O, Torgan E, Karadag R. The characterisation by liquid chromatography of lake pigments prepared from European buckthorn (*Rhamnus cathartica* L.). Pigment Resin Technol 2012;41:331–8. https://doi.org/10.1108/03699421211274234.
[42] Lech K, Fornal E. A mass spectrometry-based approach for characterization of red, blue, and purple natural dyes. Molecules 2020;25:3223. https://doi.org/10.3390/molecules25143223.
[43] Peets P, Vahur S, Kruve A, Haljasorg T, Herodes K, Pagano T, et al. Instrumental techniques in the analysis of natural red textile dyes. J Cult Herit 2020;42:19–27. https://doi.org/10.1016/j.culher.2019.09.002.
[44] Ren S, Hinzman AA, Kang EL, Szczesniak RD, Lu LJ. Computational and statistical analysis of metabolomics data. Metabolomics 2015;11:1492–513. https://doi.org/10.1007/s11306-015-0823-6.
[45] Vukics V, Guttman A. Structural characterization of flavonoid glycosides by multi-stage mass spectrometry. Mass Spectrom Rev 2010;29:1–16. https://doi.org/10.1002/mas.20212.
[46] Cuoco G, Mathe C, Vieillescazes C. Liquid chromatographic analysis of flavonol compounds in green fruits of three *Rhamnus* species used in Stil de grain. Microchem J 2014;115:130–7. https://doi.org/10.1016/j.microc.2014.03.006.
[47] Fabre N, Rustan I, de Hoffmann E, Quetin-Leclercq J. Determination of flavone, flavonol, and flavanone aglycones by negative ion liquid chromatography electrospray ion trap mass spectrometry. J Am Soc Mass Spectrom 2001;12:707–15. https://doi.org/10.1016/S1044-0305(01)00226-4.
[48] Mouri C, Mozaffarian V, Zhang X, Laursen R. Characterization of flavonols in plants used for textile dyeing and the significance of flavonol conjugates. Dyes Pigments 2014;100:135–41. https://doi.org/10.1016/j.dyepig.2013.08.025.
[49] Liu J, Ji L, Chen L, Pei K, Zhao P, Zhou Y, et al. Identification of yellow dyes in two wall coverings from the Palace Museum: evidence for reconstitution of artifacts. Dyes Pigments 2018;153:137–43. https://doi.org/10.1016/j.dyepig.2018.01.057.
[50] Marzouk MS, El-Toumy SAA, Merfort I, Nawwar MAM. Polyphenolic metabolites of *Rhamnus disperma*. Phytochemistry 1999;52:943–6. https://doi.org/10.1016/S0031-9422(99)00262-9.
[51] Pang H, Han Y, Sun S, Xing Z, Li L, Xia G, et al. Screening the extracts from two drying methods of *Rhamnus ussuriensis* J.J. Vassil.: assessment according to active ingredient content, antioxidant potency, and hepatoprotective effects in rats. Nat Prod Commun 2025;20. https://doi.org/10.1177/1934578X251349455. 1934578X251349455.
[52] Bourhis K, Blanc S, Mathe C, Dupin J-C, Vieillescazes C. Spectroscopic and chromatographic analysis of yellow flavonoidic lakes: quercetin chromophore. Appl Clay Sci 2011;53:598–607. https://doi.org/10.1016/j.clay.2011.05.009.
[53] Romani A, Zuccaccia C, Clementi C. An NMR and UV–visible spectroscopic study of the principal colored component of Stil de grain lake. Dyes Pigments 2006;71:218–23. https://doi.org/10.1016/j.dyepig.2005.07.005.
[54] Jiang C, Gates PJ. Systematic characterisation of the fragmentation of flavonoids using high-resolution accurate mass electrospray tandem mass spectrometry. Molecules 2024;29:5246. https://doi.org/10.3390/molecules29225246.
[55] Özipek M, Çaliş İ, Ertan M, Rüedi P. Rhamnetin 3-*p*-coumaroylrhamninoside from *Rhamnus petiolaris*. Phytochemistry 1994;37:249–53. https://doi.org/10.1016/0031-9422(94)85035-6.
[56] Sakushima A, Coşkun M, Hisada S, Nishibe S. Flavonoids from *Rhamnus pallasii*. Phytochemistry 1983;22:1677–8. https://doi.org/10.1016/0031-9422(83)80110-1.
[57] Epifano F, Genovese S, Kremer D, Randic M, Carlucci G, Locatelli M. Re-investigation of the anthraquinone pool of *Rhamnus* spp.: Madagascin from the fruits of *Rhamnus cathartica* and *R. intermedia*. Nat Prod Commun 2012;7. https://doi.org/10.1177/1934578X1200700817. 1934578X1200700817.
[58] Rosenthal I, Wolfram E, Peter S, Meier B. Validated method for the analysis of frangulins A and B and glucofrangulins A and B using HPLC and UHPLC. J Nat Prod 2014;77:489–96. https://doi.org/10.1021/np400736s.
[59] Spirydovich AV, Shabunya PS, Ahabalayeva AD, Deeva AA, Vinogradova YuK, Vlasava NB, et al. Variability of secondary metabolites in the bark of *Rhamnus cathartica* L. from native and introduced population. Dokl Akad Nauk 2025;69:40–7. https://doi.org/10.29235/1561-8323-2025-69-1-40-47.
[60] Rafaelly L, Heron S, Nowik W, Tchapla A. Optimisation of ESI-MS detection for the HPLC of anthraquinone dyes. Dyes Pigments 2008;77:191–203. https://doi.org/10.1016/j.dyepig.2007.05.007.
[61] Zhan C, Xiong A, Shen D, Yang L, Wang Z. Characterization of the principal constituents of danning tablets, a Chinese formula consisting of seven herbs, by an UPLC-DAD-MS/MS approach. Molecules 2016;21:631. https://doi.org/10.3390/molecules21050631.
[62] Villela A, van Vuuren MSA, Willemen HM, Derksen GCH, van Beek TA. Photostability of a flavonoid dye in presence of aluminium ions. Dyes Pigments 2019;162:222–31. https://doi.org/10.1016/j.dyepig.2018.10.021.